The CuO/ZnO and CuO/ZnO/biochar materials for water treatment

J Lang[1], G J F, Cruz[2] and J L Solis[3]

[1] Technical University of Ostrava, Institute of Environmental Technology, Ostrava, Czech Republic

[2] Universidad Nacional de Tumbes, Departamento de Ingeniería Forestal y Gestión Ambiental, Tumbes, Peru

[3] Universidad Nacional de Ingeniería, Facultad de Ciencias, Lima, Peru

E-mail: jaroslav.lang@vsb.cz

Abstract. The research of new materials and methods for water treatment is necessary. Two sets of materials were prepared. The one set is composed from CuO/ZnO oxides with variable content of CuO and the second set consists of its biochar impregnated counterparts. The structure and phase composition was determined using X-ray diffraction method and morphology of the materials was studied using scanning electron microscopy. The photodegradation activity and adsorption properties were tested on model pollutant – Methylene blue (MB) dye solution. The experimental kinetic of the data was analyzed using pseudo-first-order and pseudo-second-order kinetic models and the equilibrium data was evaluated using Langmuir, Freundlich and Dubinin-Radushkievic models. It was found that optimal material for photodegradation of MB is 1% CuO/ZnO oxide and for the adsorption of MB is the best material raw corn cob biochar.

1. Introduction

The rapid industrialization, urbanization and economic boom lead to increase their living standard and energetic consumption. The environmental pollution is a tax for the huge technological advance the human civilization made up to now. One of the most precious resources available to human is fresh water. The industry and households use it on daily basis in great quantities. The wastewater that it generates needs to be very thoroughly cleaned before it can be returned to the circulation. The wastewater contains a great mixture of pollutants. From heavy metals [1], phenolics [2], dyes [3], pesticides to PPCPs (pharmaceuticals and personal care products) and others [4, 5]. The waste water is treated by array of different methods. The common water treatment methods in use are filtration, adsorption, photodegradation, oxidation, flotation etc. and their combinations [6, 7].

The adsorption is a separation process. The pollutant comes in contact with the surface of the adsorbent and is attached to it. According to the nature of the bond between pollutant and adsorbent it is distinguished between physical adsorption and chemical adsorption. In the physical adsorption the attractive forces are Van der Waals forces, the pollutant-adsorbent bond is weak, the process is reversible and the pollutant can be attached in several layers to the surface. In chemical adsorption the pollutant is with adsorbent connected by chemical bond which is far stronger and adsorption is irreversible process

[8]. In the chemical adsorption the pollutant is attached to active sites (chemical groups) on the surface of the adsorbent and forms a monolayer on the adsorbent. The chemisorption is selective and by tailoring the active sites can target specific pollutant [9, 10]. The pollutant, can in some cases, be desorbed and the adsorbent reused otherwise the spent adsorbent with the pollutant has to be safely disposed of.

The important parameters for the adsorbents are specific surface area, pore size distribution and chemical composition of the surface layer. The widely used adsorbents are activated carbon, zeolites, silica, polymeric resins, etc. The activated carbon materials can be prepared from variety of carbonaceous materials like coal or from agrowaste such as corn cob, coffee husk and cocoa pod husk [3]. The materials are pyrolyzed at high temperature (above 400 °C) without oxygen and subsequently activated by oxidizing agent which helps create and access pores. The adsorption properties may be further enhanced by impregnation and functionalization. The activated carbon adsorbents adsorb organic pollutants very well but adsorption of heavy metals and metalloids (Pb, Cr, As) can be improved by impregnation with ZnO [11, 12].

Photodegradation is a process where the photoactive material is used for chemical degradation of pollutants. The photocatalyst materials are able to absorb photons of UV and visible light and utilize their energy to produce reactive chemical species such as OH^* and O_2^{-*} reactive radicals. These species cannot exist alone for a prolonged time and for the purposes of the photodegradation of pollutants need to be continually generated. The photodegradation does not necessarily lead to complete mineralization of the pollutant to complete degradation to H_2O, CO_2 and inorganic salts. The photodegradation process should be monitored and adjusted to prevent formation of products that are harmful or possibly even more toxic than the initial pollutant. The process is not selective and is sensitive to turbidity. The photocatalyst if properly anchored can be used repeatedly [13].

The biochar is carbonaceous material with significantly lower specific surface area than activated carbon but much easier and eco-friendly synthesis. It can be produced from agrowaste and its adsorption properties can be enhanced by impregnation. The agrowastes disposal is a problematic issue in many countries. Annually, tons of agrowastes are generated and burned or dumped over. The other problem plaguing developing countries is water pollution. The utilization of the agrowaste for the biochar production is trying to help solve both problems. This paper aims at demonstrating two different methods for water treatment and dealing with model pollutant - Methylene blue (MB). The Methylene blue is dye from phenothiazine family it is widely used in chemistry and medicine and in this work will serve as a model organic pollutant. The two chosen degradation/separation methods were demonstrated on two sets of samples: the set of mixed oxides 1% CuO/ZnO, 5% CuO/ZnO, 10% CuO/ZnO was used in photoactivity testing and the set of mixed oxides impregnated on biochar was used for adsorption tests.

2. Experimental

Two sets of materials were prepared. The first set was supposed to compose of three different mixtures of CuO and ZnO with the CuO content varied from 1 mol% to 5 mol% and 10 mol% of CuO in ZnO.

The second set is composed of three CuO and ZnO mixturers impregnated to biochar. The CuO and ZnO mixtures are of the same composition as in the first set.

2.1. *Metal oxides*

The solution of NaOH (c=0.5 M) was heated to 60°C and dropwise was added Copper acetate (c=0.33 M) and $Zn(NO_3)_2$ (c=0.5 M) from two separate burets. The temperature was raised to 80°C and kept for 2 h. The suspension was then sonicated for 30 min, centrifuged and dried in oven for 24 h at 60 °C. The materials were marked as 1% CuO/ZnO, 5% CuO/ZnO, and 10% CuO/ZnO.

2.2. *Metal oxide impregnated biochar*

The biochar was prepared by pyrolysis of agrowaste corn cob (particle size <0.5 mm) at 600 °C for 2 h under nitrogen flux (150 ml·min⁻¹). The biochar was subsequently washed with 0.5 M HCl, hot and cold distilled water. The washed biochar was then dried in oven for 24 h at 100°C. The biochar impregnation was done the same way as the synthesis of metal oxides above. The biochar was mixed with the sodium

hydroxide solution and the rest of the procedure was the same. The product was sonicated for 30 min, washed with distilled water, filtered and dried in oven for 24 h at 60 °C. The composites were marked as 1% CuO/ZnO/Biochar, 5% CuO/ZnO/Biochar, and 10% CuO/ZnO/Biochar.

2.3. Characterization

The phase and crystallinity were studied by X-ray diffraction (XRD) using Bruker D8 Advance diffractometer operated at 40 kV and 40 mA, with CuKα (λ=1.5406 Å) radiation. The XRD patterns were collected in a 2Θ range from 5° to 80° and analyzed using software Match!

The field emission scanning electron microscope (FSEM) Rigaku SU8230 was used for characterization of the morphology of the studied adsorbents. The absorbance of Methylene blue (MB) solution used in adsorption and photodegradation experiments was determined using UV-vis spectrometer Perkin Elmer Lambda 365 in 10 mm quartz glass cuvettes. The adsorption properties of the biochar composites were tested using equilibrium and kinetic adsorption tests with Methylene blue. The photoactivity of the oxide materials was tested with photodegradation test with Methylene blue.

2.4. Equilibrium adsorption tests

The equilibrium experiments were performed using nine different initial solutions of Methylene blue (MB): 5, 10, 20, 50, 100, 150, 200, 300 and 400 mg·L^{-1}. The total solution volume was 50 ml and was added 0.1 g of the adsorbent into every solution. The time to reach the equilibrium stage was 24 h. The initial pH level was measured for every solution. The models of adsorption isotherm applied to the equilibrium data were Langmuir, Freundlich and Dubinnin-Raduskevich. The equilibrium adsorption uptake of MB on the adsorbents, q_e (mg·g^{-1}) were calculated using the following equation:

$$q_e = \frac{(C_0 - C_e)V}{m_{BC}} \tag{1}$$

where C_0 (mg·L^{-1}) and C_e (mg·L^{-1}) are initial concentration and the concentration at equilibrium, respectively. V (L) is the volume of the solution and m_{BC} (g) is the amount of biochar added.

The Langmuir model:

$$q_e = \frac{Q_0 \cdot K_L \cdot C_e}{1 + K_L \cdot C_e} \tag{2}$$

where C_e (mg·L^{-1}) is adsorbate concentration at equilibrium, q_e (mg·g^{-1}) is the amount of adsorbate uptake at equilibrium. K_L (L·mg^{-1}) is Langmuir equilibrium constant, Q_0 (mg·g^{-1}) is saturated monolayer adsorption capacity of adsorbent.

Freundlich model:

$$q_e = K_F \cdot C_e^n \tag{3}$$

where the K_F (mg·g^{-1})/(mg·L^{-1})^n is Freundlich constant. The n (dimensionless) is Freundlich intensity parameter.

Dubinin-Radushkievic model:

$$q_e = q_{DR} \cdot e_e^{-K_{DR} \cdot \varepsilon^2} \tag{4}$$

where q_{DR} (mg·g^{-1}) and K_{DR} (mol^2·kJ^{-2}) are Dubinin-Radushkevic constants, ε is a Polanyii potential.

2.5. Kinetic adsorption tests

Kinetic experiments were conducted using initial MB concentration of 10 mg·L^{-1} (150 mL of total solution) and biochar load of 0.5 g, the pH level was adjusted between 9 – 9.5. Aliquots (approx. 5 ml) were taken at the beginning, 2, 4, 6, 8, 10, 15, 20, 25, 30, 45, 60, 75, 90 and 120 min. Every aliquot was filtered through 0.45 µm filter and the concentration of MB determined using UV-vis spectrometer. The amount of MB adsorbed at time t was calculated by using the following mass balance equation:

$$q_t = \frac{(C_0 - C_t)V}{m_{BC}} \tag{5}$$

where C_0 is the initial concentration of MB and C_t is the MB concentration in solution at time t (mg L^{-1}). V is the total volume of solution (L) and m_{BC} is the mass of biochar.

The nonlinear pseudo-first-order rate equation (PFO):

$$q_t = q_e \cdot \left(1 - e^{-k_1 \cdot t}\right) \tag{6}$$

where q_e (mg·g^{-1}) and q_t (mg·g^{-1}) are the amounts of MB sorbed at equilibrium and at time t. The k_1 (min^{-1}) is the rate constant of the PFO equation.

The nonlinear pseudo-second-order rate equation (PSO):

$$q_t = \frac{q_e^2 \cdot k_2 \cdot t}{1 + k_2 \cdot q_e \cdot t} \tag{7}$$

where k_2 (g·mg^{-1}·min^{-1}) is the rate constant of the PSO equation.

2.6. Photoactivity test

Photocatalytic activity of prepared materials was assessed from the degradation of Methylene blue dye solution. The CuO/ZnO oxides under UV-vis light (Ultra-Vitalux OSRAM 220 V, 300 W) degraded Methylene blue dye (with absorption maximum at 664 nm) and decreased the concentration of the solution. This concentration was monitored from the absorption intensity of the solution. The measurement was performed on a UV-vis spectrometer in 10 mm quartz glass cuvettes.

The layout of the experiment: The 0.05 g of the powder material was mixed with 150 mL of MB solution (c = 10 mg·L^{-1}). The suspension was stirred (400 rpm) for 30 min in dark. Aliquots (approx. 5 mL) were taken at the beginning, 5, 10, 15, 20, 25, 30, 60, 90 and 120 min. Every aliquot was filtered through 0.45 µm filter. Two millilitres of the filtered solution were diluted with distilled water to 25 mL solution and the absorbance was measured on this dilute solution.

Prior to the photodegradation experiments, the calibration curve was determined using different concentrations of MB solution (0.00, 0.10, 0.19, 0.38, 0.58, 0.77, 1.15 ppm). The regression curve from calibration data was used to determine the concentration of the dye from the measured absorbance (8).

$$A = 0.186 \cdot c + 0.0019 \tag{8}$$

where A is an absorbance and c is a concentration (ppm).

Evaluation of kinetic data (determination of rate constants): Photocatalytic activity of prepared material was expressed as conversion of MB (X_{MB}) dependent on time according to equation (9):

$$X_{MB} = \frac{c_{0(MB)} - c_{(MB)}}{c_{0(MB)}} \cdot 100 \tag{9}$$

First-order rate-constant was obtained from the linear regression:

$$\ln\left(\frac{c_0}{c}\right) = k \cdot t \tag{10}$$

where c_0 is initial concentration (mol·L^{-1}) and c (mol·L^{-1}) is concentration at the time t, k is a rate constant (min^{-1}), t is a time (min).

For the purpose of comparison of the adsorption and photoactivity the q_{pd} (mg·g^{-1}) was devised and represents the weight of the MB dye photodegraded per weight of the photocatalyst.

$$q_{pd} = \frac{c_{0(MB)} \cdot V_{(MB)} \cdot \frac{X}{100}}{m_{(photocatalyst)}} \tag{11}$$

Where c_0 is the initial concentration (mg·L^{-1}), V_{MB} is the volume of the solution (L), X is a conversion (%) and $m_{(photocatalyst)}$ is the weight of the photocatalyst material (g).

3. Results and discussion

The structure of the materials was analyzed using XRD. The diffractograms are shown in Figure 1. The phase composition is in both materials very similar. The three major phases are Garhardtite ($Cu_2H_3NO_6$, Match! Refpattern_96-901-2716), Zincite (ZnO, Match! Refpattern_96-900-4180) and CuO (Match! Refpattern_96-410-5686). The two large peaks in Figure 1 b) at positions from 18 to 30° and from 40 to 50° are typical for carbonaceous materials such as biochar. The oxides in diffractogram 1 a) show better crystallinity.
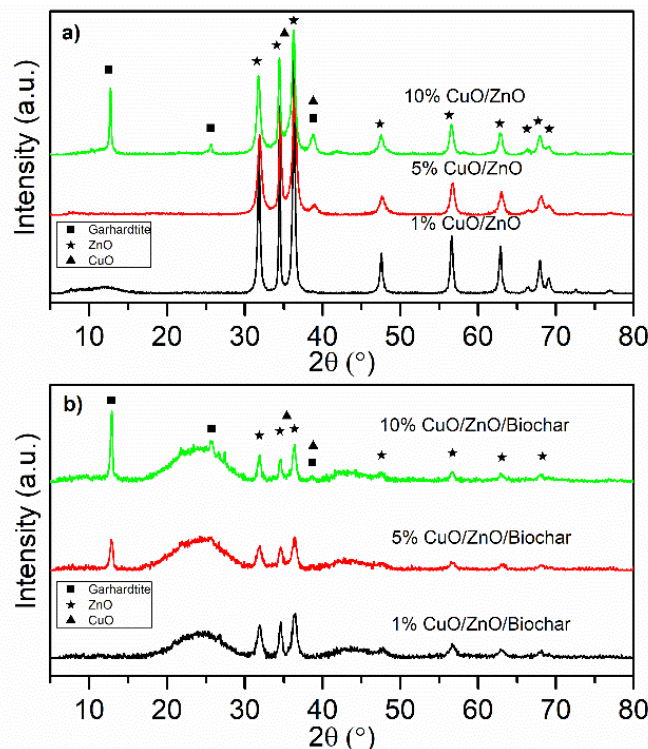

Figure 1. The XRD diffractograms of a) CuO/ZnO oxides and b) CuO/ZnO/Biochars.

The morphology of the materials was examined by SEM as shown in Figure 2. The biochar particles shown in Figure 2 a) are 10 to 20 µm large. The Figure 2 b, c, d) show anchored oxides on the biochar particles. The oxide particles in Figure 2 b-f) are sponge-like agglomerates of very small crystallites. The thin platelet/sheet particles found in 2 c, d) suggest the biochar was during the impregnation process exfoliated or delaminated.
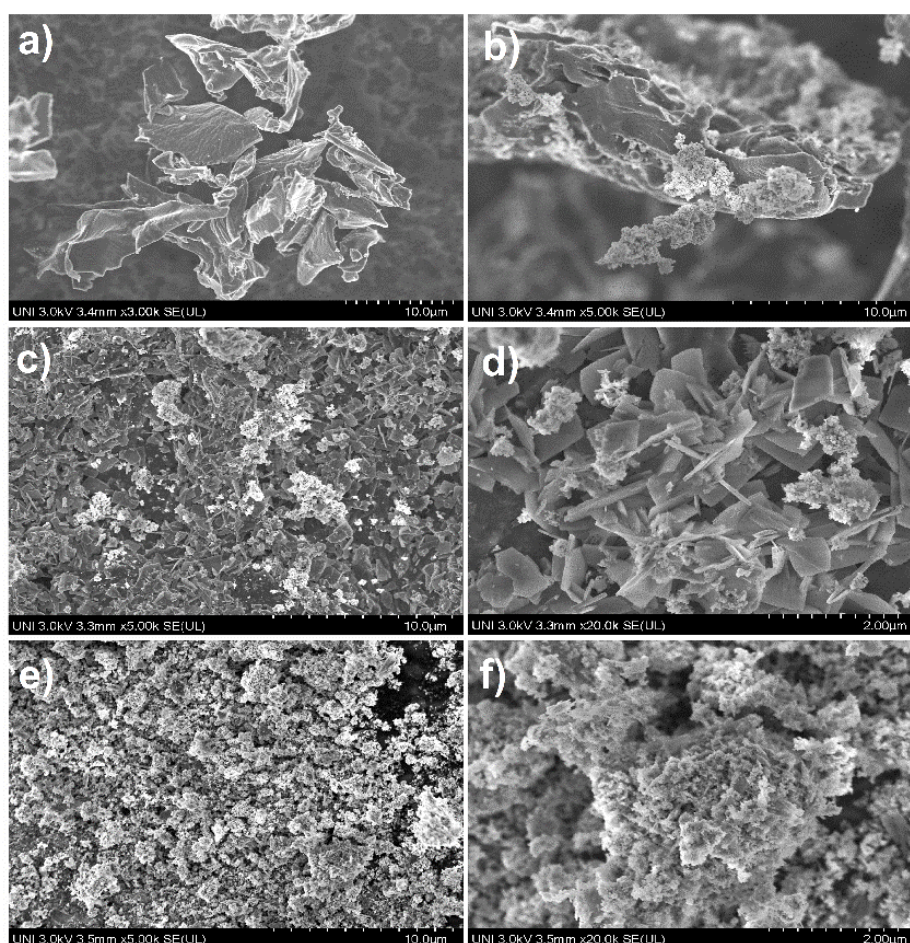
Figure 2. The SEM images of a) Biochar, b) 1% CuO/ZnO/Biochar, c, d) 10% CuO/ZnO/Biochar, e, f) 1% CuO/ZnO.

The kinetic adsorption test (Fig. 3) showed good affinity of MB to the biochar composite materials, the equilibrium in the kinetic test is established in less than two minutes. The highest sorption capacity q_t in the kinetic test is recorded for the raw biochar (Fig. 3 a)). From the comparison of coefficients of determination R^2 and chi-square statistic χ^2, the MB kinetic test data were best fitted with Pseudo first order model ($R^2 = 0.87$-0.97 and $\chi^2 = 0.00$-0.05).

Table 1. The kinetic test.

Kinetic rate equation	Material	Q_e (mg·g^{-1})	k_1 (min^{-1})	χ^2	R^2
PFO	Biochar	1.91	39016.39	0.05	0.87
	1% CuO/ZnO/Biochar	1.55	988.23	0.01	0.97
	5% CuO/ZnO/Biochar	1.24	6083.13	0.01	0.95
	10% CuO/ZnO/Biochar	1.32	21.69	0.00	0.97

The PSO parameters were negative and are not shown in the table as the model proved to be unsuitable for this data.
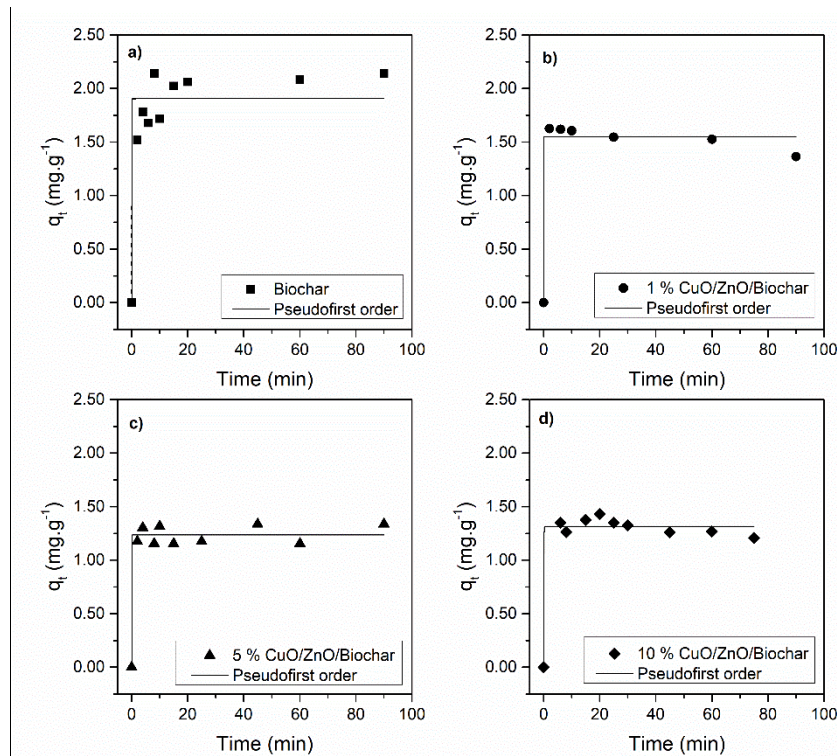
Figure 3. MB kinetic data by CuO/ZnO/Biochar materials.

In the equilibrium adsorption test the highest adsorption capacity for MB showed raw biochar (Fig. 4a)). The adsorption capacity of the raw biochar surpassed all of the biochar composite materials. The equilibrium was achieved only with 5% CuO/ZnO/Biochar material (q_e = 5.08 mg·L^{-1}, C_e = 153.38 mg·g^{-1}). Although the equilibrium concentration was not reached in the case of raw biochar it can be said it surpassed all other tested materials in MB equilibrium adsorption test. From the comparison of coefficients of determination R^2 and chi-square statistic χ^2, the MB equilibrium test data (Table 2) were best fitted with Langmuir model (R^2 = 0.92-0.98 and χ^2 =0.08-0.92).

Table 2. The equilibrium test.

| Model	Material	Q_0 (mg·g^{-1})	K_L (L·mg^{-1})	χ^2	R^2
Langmuir	Biochar	12.91	0.05	0.72	0.96
	1% CuO/ZnO/Biochar	9.62	0.04	0.92	0.92
	5% CuO/ZnO/Biochar	5.62	0.04	0.08	0.97
	10% CuO/ZnO/Biochar	7.38	0.04	0.14	0.98
		K_F (mg·g^{-1})/(mg·L^{-1})^n	n (-)	χ^2	R^2
Freundlich	Biochar	2.26	0.29	1.44	0.93
	1% CuO/ZnO/Biochar	1.63	0.30	1.05	0.90
	5% CuO/ZnO/Biochar	0.94	0.31	0.42	0.86
	10% CuO/ZnO/Biochar	1.24	0.31	0.80	0.86
		q_{DR} (mg·g^{-1})	k_{DR} (mol^2·kJ^{-2})	χ^2	R^2
Dubinin-Raduskevic	Biochar	10.91	15.42	3.67	0.82
	1% CuO/ZnO/Biochar	8.12	18.62	2.54	0.77
	5% CuO/ZnO/Biochar	4.82	42.59	0.44	0.86
	10% CuO/ZnO/Biochar	6.02	19.29	0.95	0.83
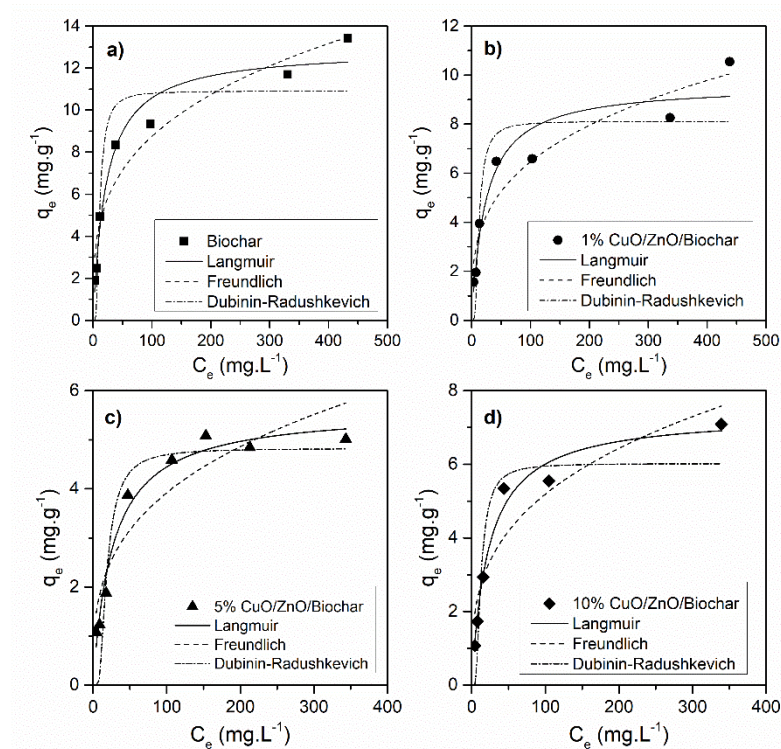
Figure 4. MB adsorption isotherms by CuO/ZnO/Biochar materials.
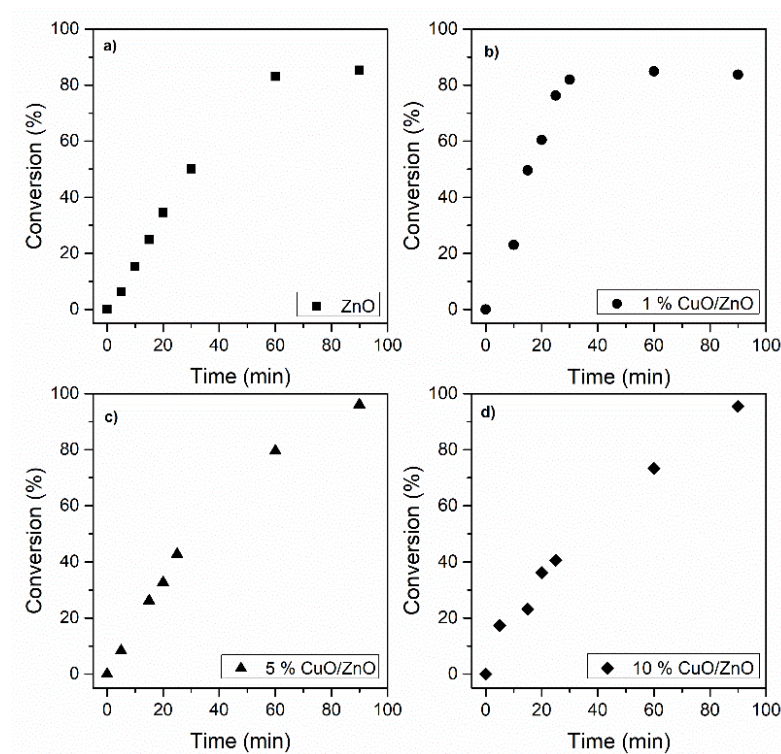

Figure 5. The comparison of conversions achieved in photoactivity test with MB and CuO/ZnO materials.

Table 3. The photoactivity test results.

Material	$k \cdot 10^2$ (min^{-1})	X_{MB} $(\%)^a$	q_{pd} $(mg.g^{-1})$
ZnO	3.02±0.17	85	25.50
1% CuO/ZnO/Biochar	7.36±0.28	90	27.00
5 % CuO/ZnO/Biochar	3.52±0.28	96	28.80
10 % CuO/ZnO/Biochar	3.51±0.26	98	29.40
^{a}Maximum conversion achieved in 90 minutes.			

The biochar composites showed increased conversion of MB (Figure 5) in comparison to the ZnO. The kinetic equation of photocatalytic degradation of Methylene blue with CuO/ZnO oxide materials is of pseudofirst order. Although the increased content of CuO hindred the photoactivity performance, the 1% CuO/ZnO shows improvement in comparison to pure ZnO. The 1% CuO in ZnO proportion appears to be optimal.

The metal oxide synthesis and impregnation process affects the morphology of the biochar. The particles of the impregnated biochar were significantly smaller compared to the raw/untreated biochar and the prevailing shape among them was of thin platelets or sheets. The most probable cause is exfoliation of biochar due to exposition to the NaOH or the ultrasonication during the impregnation.

Although the equilibrium in the equilibrium adsorption test was achieved only with one material, it provides enough data for comparison of the materials.

In the photodegradation test, the best conversion was achieved by 98 % after 90 min, but with the 1 % CuO/ZnO was achieved conversion 90 % in just 30 min, which is only 8 % lower but 3 times quicker.

If we want to compare the degradation/separation of MB by adsorption and photodegradation we need to consider the adsorbed/degraded amount of MB per gram of the material and take into account the time. The photodegradation test and kinetic adsorption test both used the MB concentration of 10 mg·L^{-1} and lasted 90 min. If we focus on the best materials in both sets (raw biochar and 1% CuO/ZnO) and take a look at q_{pd} and Q_e (PFO) we see that the q_{pd} is more than 12 times higher than Q_e (PFO). The same amount of 1% CuO/ZnO photodegradaded more than 12 times the amount of MB that was adsorbed on raw biochar in 90 mins. If we consider that 1% CuO/ZnO achieved 90% conversion in just 30 min it is a significant difference. It is important to note that the metal oxide impregnation of biochar is usually used to improve adsorption of metal ions (such as Pb, As, Cd) from the water environment and in the case of MB it probably screens the active sites and pores at the surface and hinders the adsorption. With a different pollutant the results could be diametrically different. The purpose of this paper is only to illustrate different methods of water treatment not to compare them.

4. Conclusions

The photodegradation and adsorption of MB on the prepared materials demonstrated two methods for combating pollution and illustrated the need to study and tailor the water treatment methods to the type of pollutants. The optimal material for photodegradation of MB was 1% CuO/ZnO oxide material. The impregnation of corn cob biochar with CuO/ZnO did not lead to improvement in the adsorption of MB. Further tests with the corn cob biochar adsorption should use different pollutants. To compare the two methods the tests should be run on the same set of materials and more pollutants should be tested.

References

[1] Alkurdi S S A, Herath I, Bundschuh J, Al-Juboori R A, Vithanage M, Mohan D 2019 Biochar versus bone char for a sustainable inorganic arsenic mitigation in water: What needs to be done in future research? *Environ Int* **127** 52-69

[2] Ryu J, Kim W, Kim J, Ju J, Kim J 2017 Is surface fluorination of TiO_2 effective for water purification? The degradation vs. mineralization of phenolic pollutants. *Catalysis Today* **282** 24-30

[3] Nethaji S, Sivasamy A, Mandal A B 2013 Adsorption isotherms, kinetics and mechanism for the adsorption of cationic and anionic dyes onto carbonaceous particles prepared from Juglans regia shell biomass. *International Journal of Environmental Science and Technology* **10** 231-42

[4] Couto C F, Lange L C, Amaral M C S 2019 Occurrence, fate and removal of pharmaceutically active compounds (PhACs) in water and wastewater treatment plants—A review. *Journal of Water Process Engineering* **32** 100927

[5] Quesada H B, Baptista A T A, Cusioli L F, Seibert D, de Oliveira Bezerra C, Bergamasco R 2019 Surface water pollution by pharmaceuticals and an alternative of removal by low-cost adsorbents: A review. *Chemosphere* **222** 766-80

[6] Al-Ghouti M A, Al-Kaabi M A, Ashfaq M Y, Da'na D A 2019 Produced water characteristics, treatment and reuse: A review. *Journal of Water Process Engineering* **28** 222-39

[7] Pichel N, Vivar M, Fuentes M 2019 The problem of drinking water access: A review of disinfection technologies with an emphasis on solar treatment methods. *Chemosphere* **218** 1014-30

[8] Tran H N, You S-J, Chao H-P 2016 Thermodynamic parameters of cadmium adsorption onto orange peel calculated from various methods: A comparison study. *Journal of Environmental Chemical Engineering* **4**(3) 2671-82

[9] Aljeboree A M, Alshirifi A N, Alkaim A F 2017 Kinetics and equilibrium study for the adsorption of textile dyes on coconut shell activated carbon. *Arabian Journal of Chemistry* **10** 3381-93

[10] Saruchi, Kumar V 2019 Adsorption kinetics and isotherms for the removal of rhodamine B dye and Pb^{+2} ions from aqueous solutions by a hybrid ion-exchanger. *Arabian Journal of Chemistry* **12**(3) 316-29

[11] Li C, Zhang L, Gao Y, Li A 2018 Facile synthesis of nano ZnO/ZnS modified biochar by directly pyrolyzing of zinc contaminated corn stover for Pb(II), Cu(II) and Cr(VI) removals. *Waste Manag* **79** 625-37

[12] Chen M, Bao C, Hu D, Jin X, Huang Q 2019 Facile and low-cost fabrication of ZnO/biochar nanocomposites from jute fibers for efficient and stable photodegradation of methylene blue dye. *Journal of Analytical and Applied Pyrolysis* **139** 319-32

[13] Khataee A R, Kasiri M B 2010 Photocatalytic degradation of organic dyes in the presence of nanostructured titanium dioxide: Influence of the chemical structure of dyes. *Journal of Molecular Catalysis A: Chemical* **328**(1-2) 8-26